DRAG FORCE ON MICROWAVE ANTENNA

by

J. E. Cermak[1]
J. A. Peterka[2]
B. Bienkiewicz[3]
and
N. Hosoya[4]

FLUID MECHANICS AND
WIND ENGINEERING PROGRAM

COLLEGE OF ENGINEERING

COLORADO STATE UNIVERSITY
FORT COLLINS, COLORADO

DRAG FORCE ON MICROWAVE ANTENNA

by

J. E. Cermak[1]
J. A. Peterka[2]
B. Bienkiewicz[3]
and
N. Hosoya[4]

for

Gabrial Electronics, Inc.
P.O. Box 626
Scarborough, Maine 04074

Fluid Mechanical and Wind Engineering Program
Fluid Dynamics and Diffusion Laboratory
Department of Civil Engineering
Colorado State University
Fort Collins, CO 80523

CSU Project 2-95380

December 1983

[1]Professor-in-Charge, Fluid Mechanics and Wind Engineering Program

[2]Associate Professor

[3]Assistant Professor

[4]Graduate Research Assistant

CER83-84JEC-JAP-BB-NH29

TABLE OF CONTENTS

LIST OF FIGURES

LIST OF TABLES

LIST OF SYMBOLS

Symbol

A	reference area
C_D	drag coefficient
C_DA	product of drag coefficient C_D and reference area A
F_D	drag force
L_m	typical length for model
L_p	typical length for prototype
U	wind speed
α	wind direction
λ_L	geometric scale (= L_m/L_p)
ρ	density of air

1. INTRODUCTION

Wind induced loads are important parameters to be evaluated during structural analysis of microwave antennas. Theoretical prediction of the wind forces exerted on such structures is practically impossible due to a complex nature of a separated flow. The wind forces suggested in ANSI Standard (1) are inaccurate because of absence of considerations regarding geometric details for a specific antenna. As a result, the realistic wind forces must be based on the data obtained from the wind tunnel tests.

Hoerner (2) collected data related to the drag on various bluff bodies. Some of these data can be used to estimate the drag force of a microwave horn antenna. Wind tunnel tests of horn antennas were reported by Kamei, Kimura and Matsushita (3), Poreh and Cermak (4), and Cermak et al. (5).

Cermak et al. (5) compared the drag force measured for different antennas and found that the Gabrial UHR10 D antenna (shown in Figure 1) exhibited the largest drag force. The objective of the wind tunnel study presented herein was to re-evaluate the mean drag force on the Gabrial UHR10 D antenna. The original geometry of the antenna was modified and the drag force was measured. The results for the modified geometry was compared with the data presented by Cermak et al. (5).

2. EXPERIMENTAL PRELIMINARIES

2.1 Similarity Requirements

Investigation of wind effects on structures are usually considered for strong wind conditions where thermal stratification of the atmosphere is destroyed by intense vertical mixing (6). Such flow conditions were modeled for the wind tunnel study described in this report.

The essential requirements for the physical modeling included geometric similarity for the model and the prototype antenna, and dynamic similarity for the flow.

Geometric similarity was easily achieved by an undistorted scaling of the model geometry. Thus,

$$\frac{L_m}{L_p} = \lambda_L = \text{constant}$$

where L_m and L_p are typical lengths, respectively, for model and prototype structures.

Generally, dynamic similarity of the flow requires equality of the Reynolds numbers for model and prototype fields. However, the drag coefficient of bluff structures becomes invariant under sufficiently high Reynolds numbers (higher than critical) found in the atmospheric boundary layer (7). The value of the critical Reynolds number was examined in the preceding study (5) for an antenna of a shape and a size similar to the antenna tested in the present study. The results from Ref. (5) are reproduced in Figure 2. The data show that the drag coefficient remains constant when the wind speed exceeds 40 fps. The wind speed in the current study was then determined to be 50 fps.

2.2 Definition of Wind Load--Mean Drag Force

Time averaged drag force on a horn antenna Gabrial UHR10 D and the modified models was of particular interest in the present study. Wind-tunnel tests were performed using small-scale rigid models mounted on a platform which was also exposed to the wind. In order to evaluate the mean drag on the horn antennas, the drag contribution by the platform was separately measured and subtracted from the measured total drag on the combined structures. The net drag on the horn antenna itself shall be hereafter defined by

(the net drag on the horn antenna)
= (the drag on the horn antenna and platform)
- (the drag on the platform without the horn antenna)

The above formula is merely an approximation and no attempt was made to account for the induced drag due to flow interaction between the horn antenna and the platform.

Using a conventional notation, the drag force F_D on the horn antenna at wind direction α is schematically defined in Figure 3. The corresponding normalized drag--the drag force coefficient--is given by

$$C_D = \frac{F_D}{\frac{1}{2} \rho U^2 A}$$

where U is the wind speed, ρ is the air density, and A is the reference area, respectively. The value of A was represented by the area of the horn antenna and its mountings projected on a plane normal to the wind. Notice that the reference area varies with the wind direction as shown in Tables 1 and 2.

An alternative presentation of the drag force appears in Tables 1 and 2 as $C_D A$

$$C_D A = C_D * A$$

where A = projected area for the prototype antenna (square feet). The full-scale drag force F_D can be computed as a product of $C_D A$ and the dynamic pressure of the approach wind

$$F_D = C_D A * (\frac{1}{2} \rho U^2)$$

where ρ = air density

U = wind speed.

3. EXPERIMENTAL APPARATUS

3.1 Wind Tunnel

The experiments described in this report were conducted in the meteorological wind tunnel of the Fluid Dynamics and Diffusion Laboratory at Colorado State University. A diagram of the wind tunnel is shown in Figure 4. This closed-circuit wind tunnel is characterized by a long (96 ft) slightly diverging test section. The test section is 6 ft 8 in. wide and 6 ft hight at the location of the turntable. The ceiling is adjustable for the longitudinal pressure gradient corrections. The facility is driven by a 400HP variable pitch propeller with wind speed varying continuously from 0.5 to 100 fps.

3.2 Flow Simulation

Atmospheric conditions suggested by Cermak (6) were simulated in the wind tunnel by means of a biplanar grid placed at inlet to the wind-tunnel test section. The horn antenna model was placed 85 ft downstream of the grid at the location of the wind-tunnel turntable. Vertical profiles of the mean speed and the local turbulence intensity of the approach wind are shown in Figure 5. The data show that the flow characteristics are quite uniform in the region where the horn antennas were immersed (25 in. up to 45 in. above the wind-tunnel floor). The reference wind speed was monitored in the uniform flow region at a height of 38 in.

3.3 Model

A 1:16 geometric scale model of the upper portion of the supporting tower, the platform and horn antennas were fabricated at the Engineering Research Center Machine Shop, Colorado State University. All the geometric significance of the prototype structure was preserved.

As mentioned in the introductory section, the major objective in this wind-tunnel study was to investigate the wind effects on the horn antenna with modified geometry. Figure 1 shows the original model of the horn antenna Gabriel UHR10 D studied by Cermak et al. (5). The effects of some geometric modifications were also studied by Cermak et al. (5). They included removal of the horizontal ribs located on the back of the horn antenna, and changes of the antenna attachment (removal of one base wing). The antenna investigated in the present study was further modified by the manufacturer (Gabriel Electronics, Inc.). The antenna was attached to a platform fastened to the upper portion of the supporting tower. The tower was made of steel to provide sufficient stiffness. The platform was constructed of an aluminum plate with the full-scale dimensions of 0.69 ft by 9 ft by 18 ft.

Figure 6 is a typical view of the experimental set-up in the wind tunnel.

3.4 Data Acquisition

3.4.1 Flow Measurement

The mean wind speed and the local turbulence intensity profiles presented in Section 3.2 were measured by a single hot film probe in conjunction with a constant temperature anemometer (TSI Inc. Model 1050). The hot film probe consisted of a 0.001 in. diameter platinum sensing element of 0.02 in. in length. The probe was carried by a vertical traverse to measure the local wind speed at different heights above the wind-tunnel floor. The data were sampled for 32 seconds at a rate of 260 samples per second. The output from the hot film was fed to a data acquisition system controlled by a Hewlett-Packard System 1000 minicomputer. The data were then analyzed and stored using appropriate software.

3.4.2 Drag Measurement

A strain-gaged force balance manufactured by Inca Engineering Co. was used for the measurement of the mean drag on the horn antennas. Possible experimental error in the system was examined in detail by Poreh and Cermak (4), and was found to be ±3 percent. The force balance arrangement is shown in Figure 7.

The drag data were acquired at a rate of 260 samples per second for 16 seconds and processed with the data reduction system described above. For each measurement of the drag, the reference speed of the approach wind was simultaneously monitored by a pitot-static tube.

4. RESULTS

The results of the study are presented in Figures 8 to 12 and Tables 1 and 2. Two experiments were performed to measure C_DA for the antenna. The results of experiment number 1 (run 1) are shown in Figure 8 and Table 1. Similar data for the second experiment (run 2) are presented in Figure 9 and Table 2. The two sets of data are compared in Figure 10. The average of C_DA, computed based on Figure 10 and Tables 1 and 2 is plotted versus the wind direction in Figure 11. It is compared with the data for the original antenna in Figure 12. The C_DA data for the original antenna, Table 3 and Figure 12, was computed based on the results presented by Cermak et al. (5) (Appendix, Table A.1a, p. 108).

5. CONCLUSION

The drag force, expressed by C_DA, is lower for the modified Gabriel UHR10 D antenna by approximately 10 percent when compared with the data for the original antenna.

REFERENCES

1. American National Standards Institute, "Minimum Design Loads for Buildings and Other Structures," (1982), ANSI Standard A58.1-1982.

2. Hoerner, S. F., "Fluid-Dynamic Drag," (1965) published by Hoerner, S. F., pp. 3.17-3.18.

3. Kamei, I., E. Kimura, and I. Matsushita, "Experimental Study of Wind Force Coefficient of SHF Antennas for Telecommunication Tower Design," (1971), Proc. of the 3rd Int. Conf. on Wind Effects on Buildings and Structures, Tokyo, Japan, pp. 357-364.

4. Poreh, M. and J. E. Cermak, "Wind Forces and Moments on Microwave Antennas," (1976), Colorado State University, Report CER76-77MP-JEC12, Fort Collins, Colorado.

5. Cermak, J. E., J. A. Peterka, B.Bienkiewicz, and N. Hosoya, "Wind Forces on Microwave Antennas, Equipment and Towers," (1983), Colorado State University, Report CER82-83JEC-JAP-BB-NH43, Fort Collins, Colorado.

6. Cermak, J. E., "Laboratory Simulation of the Atmospheric Boundary Layer," (1971), AIAA Journal, Vol. 9, No. 9, pp. 1746-1754.

7. Cermak, J. E., "Aerodynamics of Buildings," (1976), Annual Review of Fluid Mechanics, Vol. 8, pp. 75-106.

FIGURES

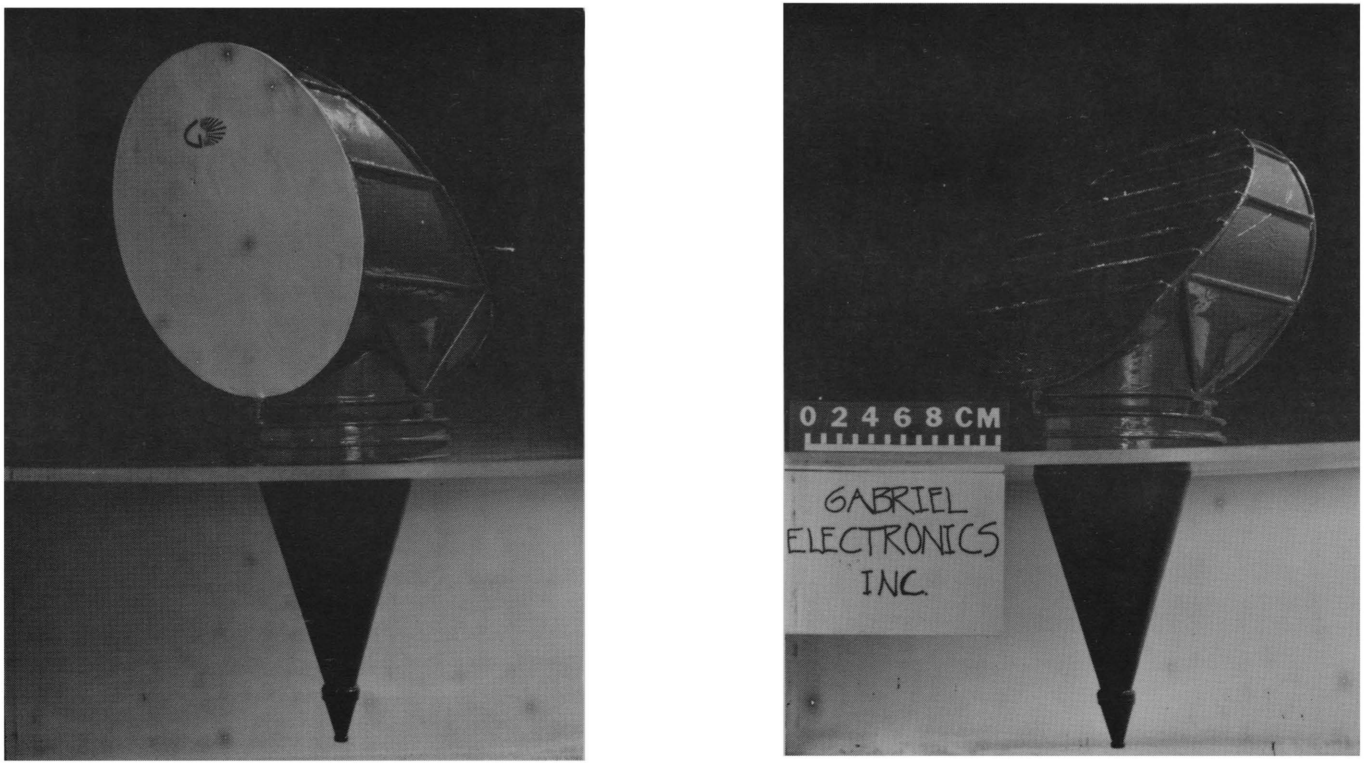

Figure 1. Conical Horn Antenna - Gabrial UHR10 D (Original Model)

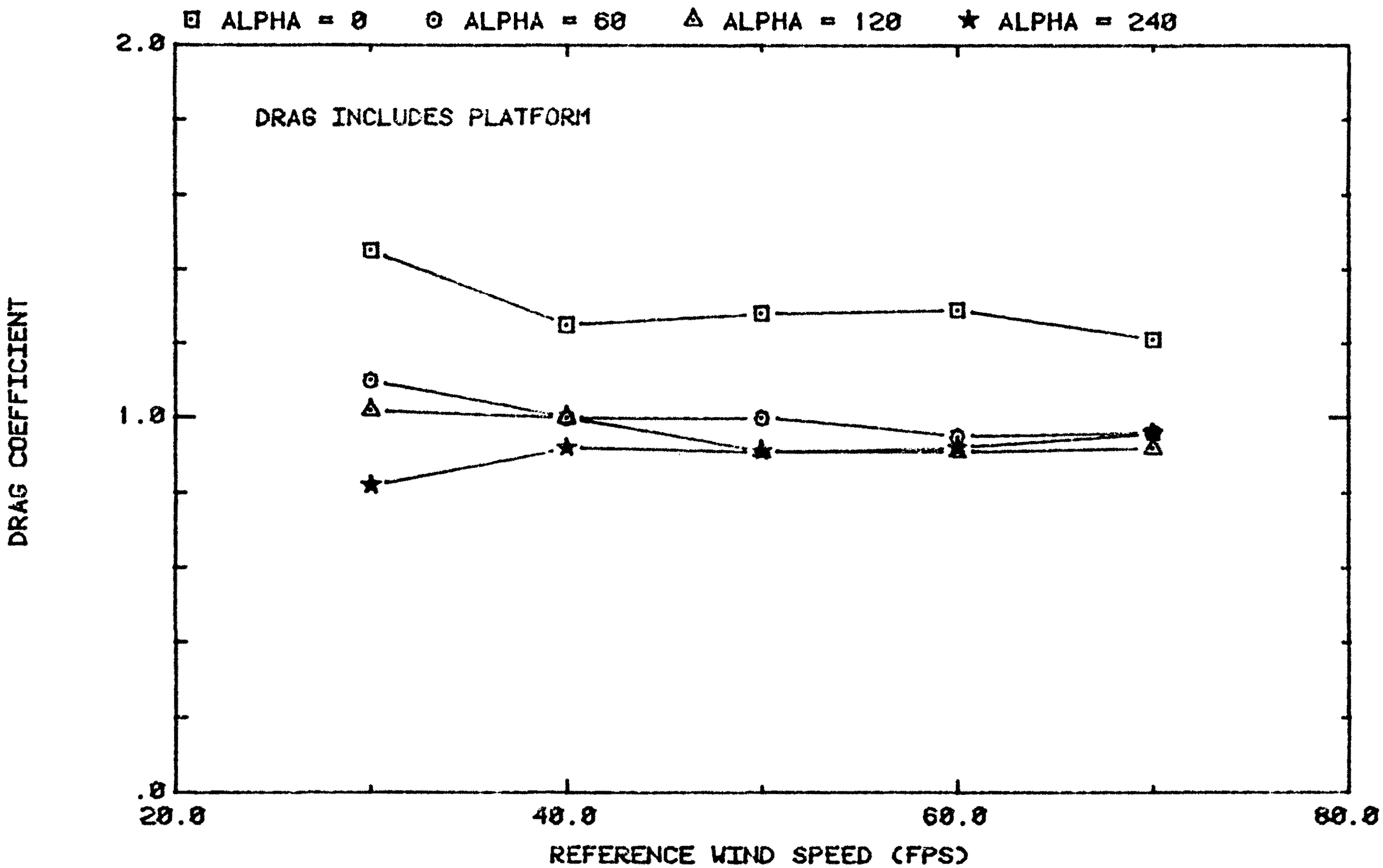

Figure 2. Effect of Wind Speed on the Drag of Conical Horn Antenna (Ref. 5)

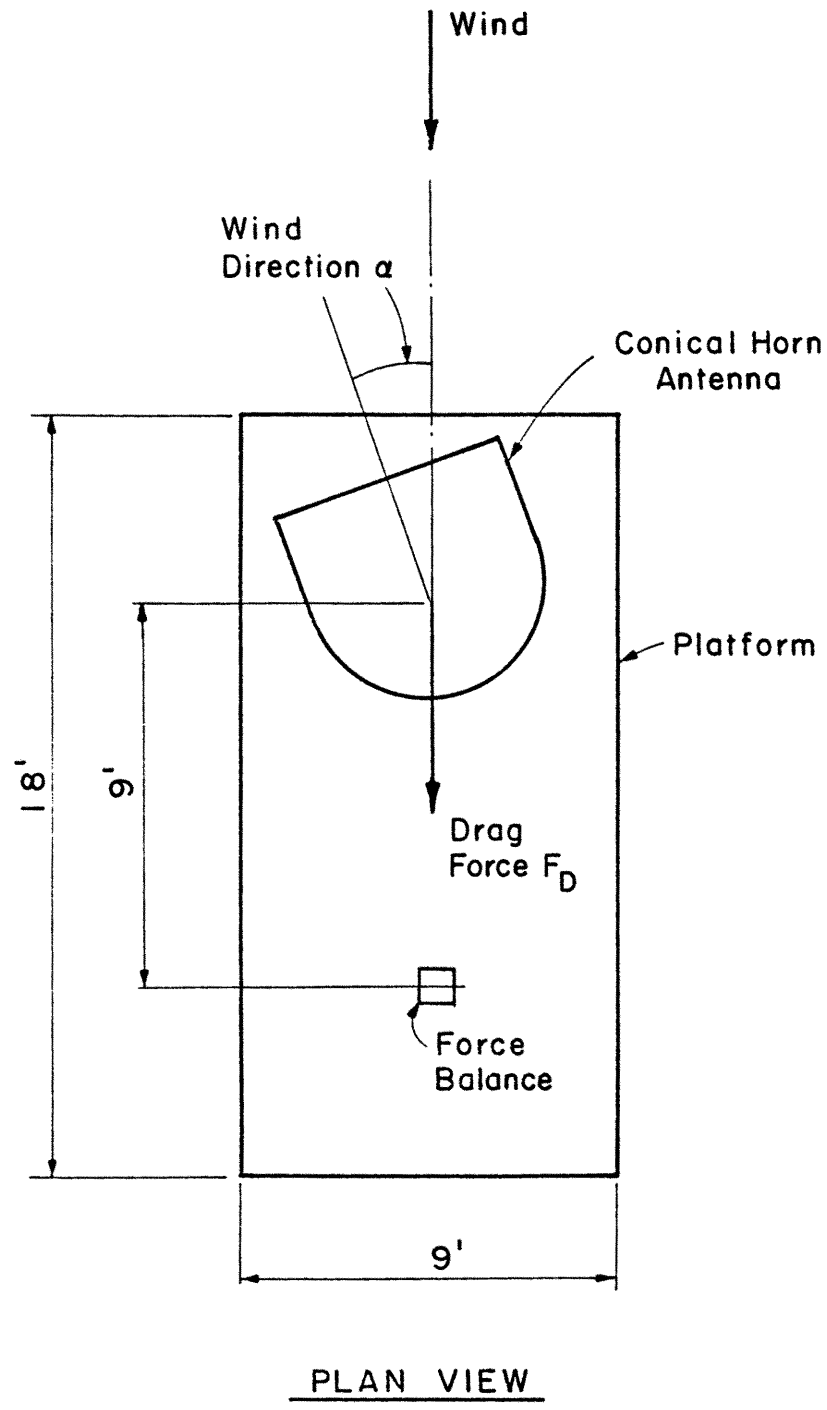

Figure 3. Definition of Drag and Wind Direction

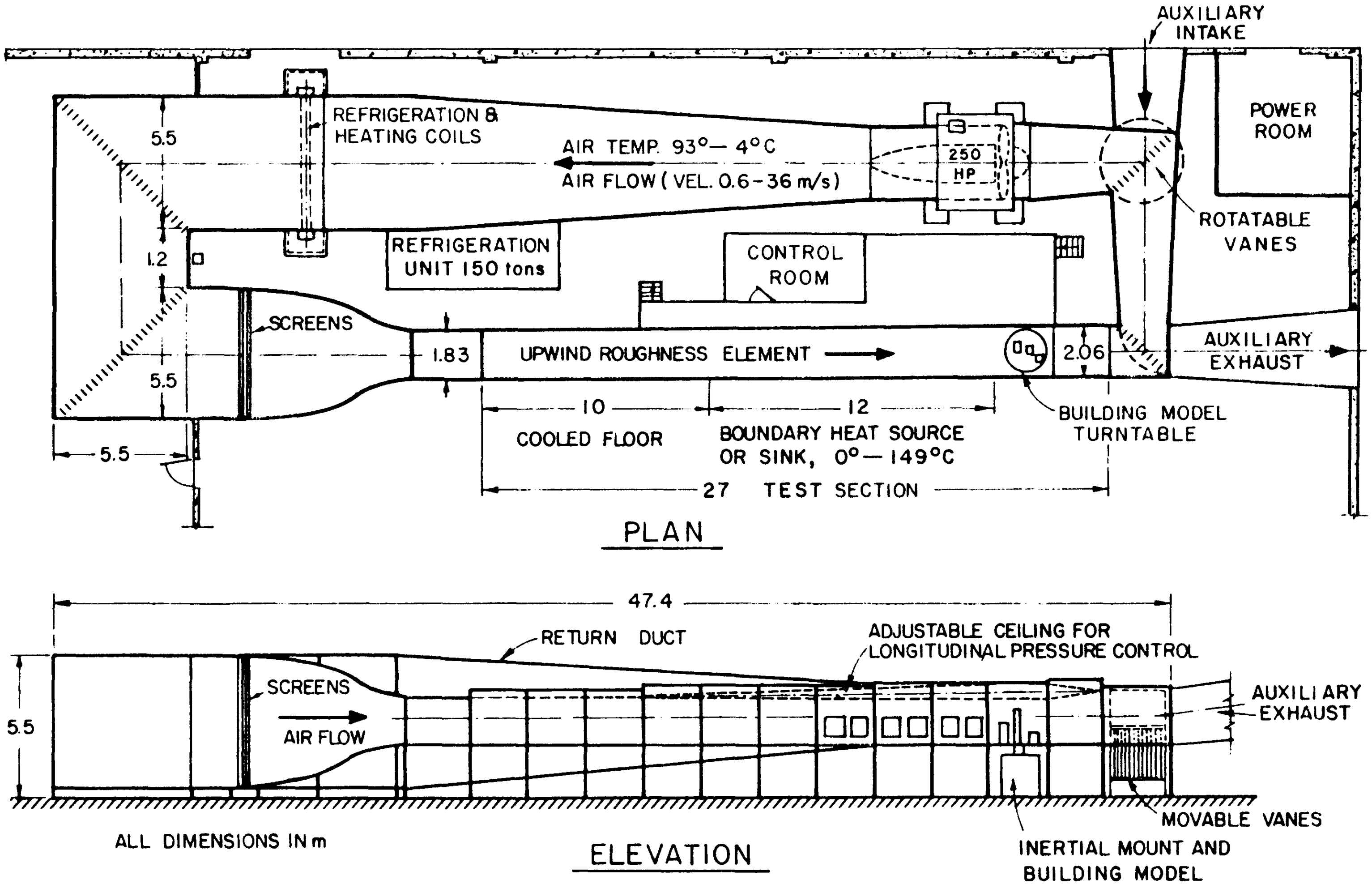

Figure 4. Meteorological Wind Tunnel

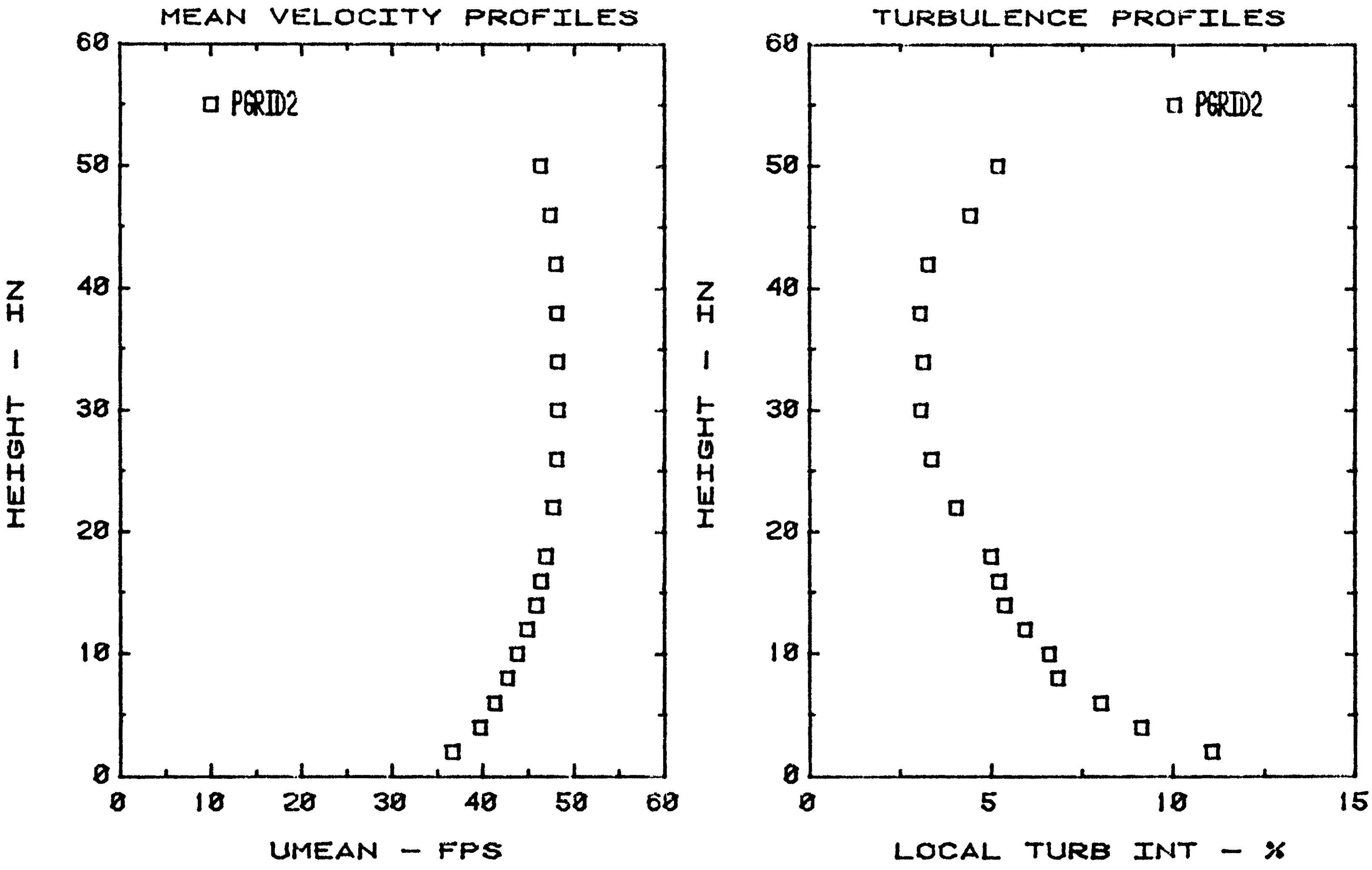

Figure 5. Wind Profile

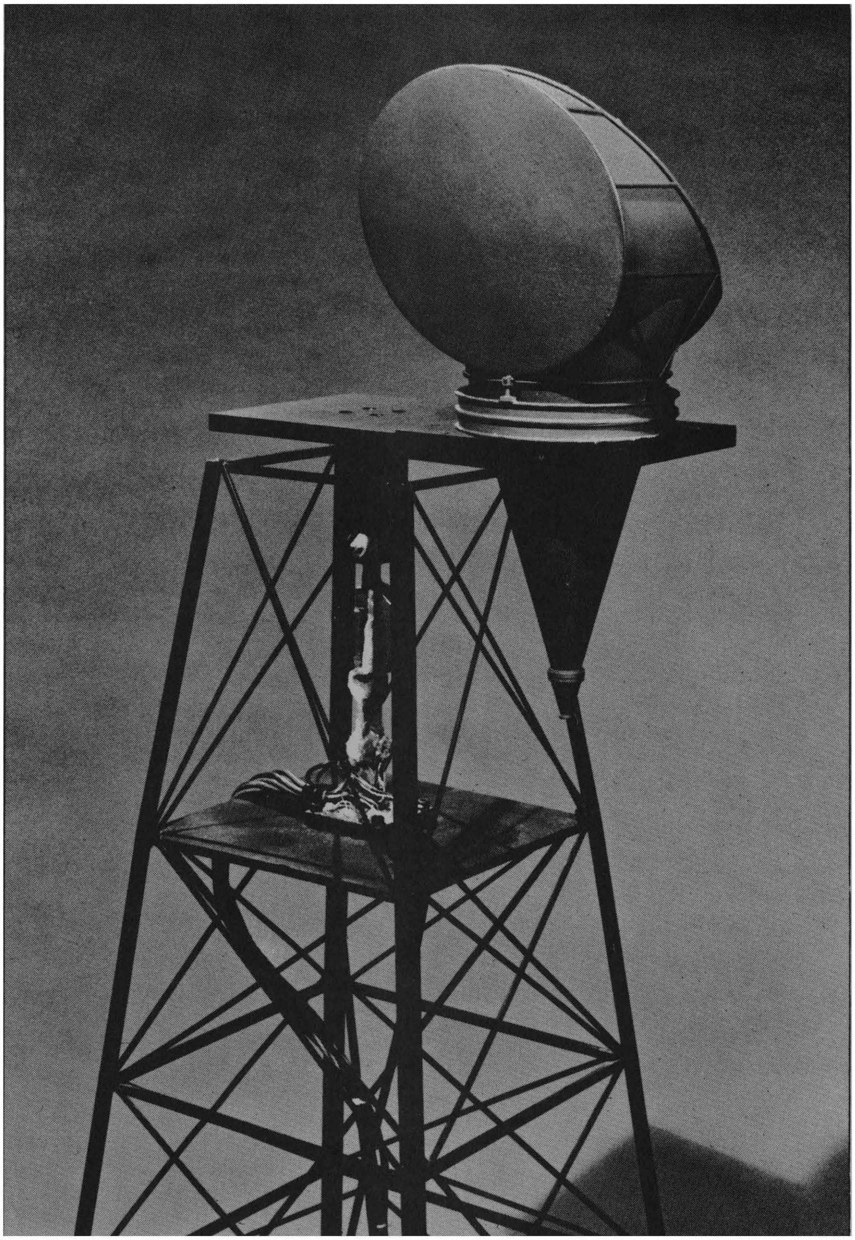

Figure 6. Conical Horn Antenna Cluster

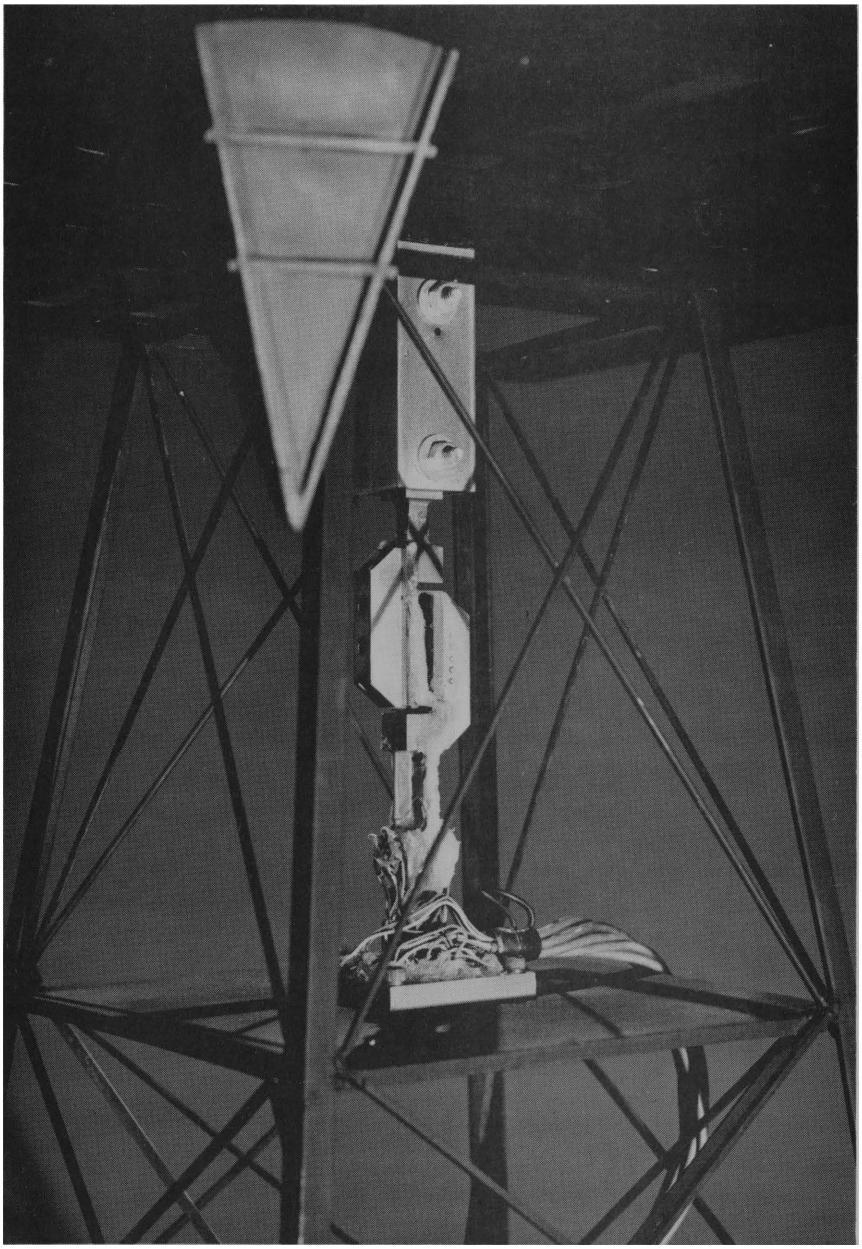

Figure 7. Force Balance Setup

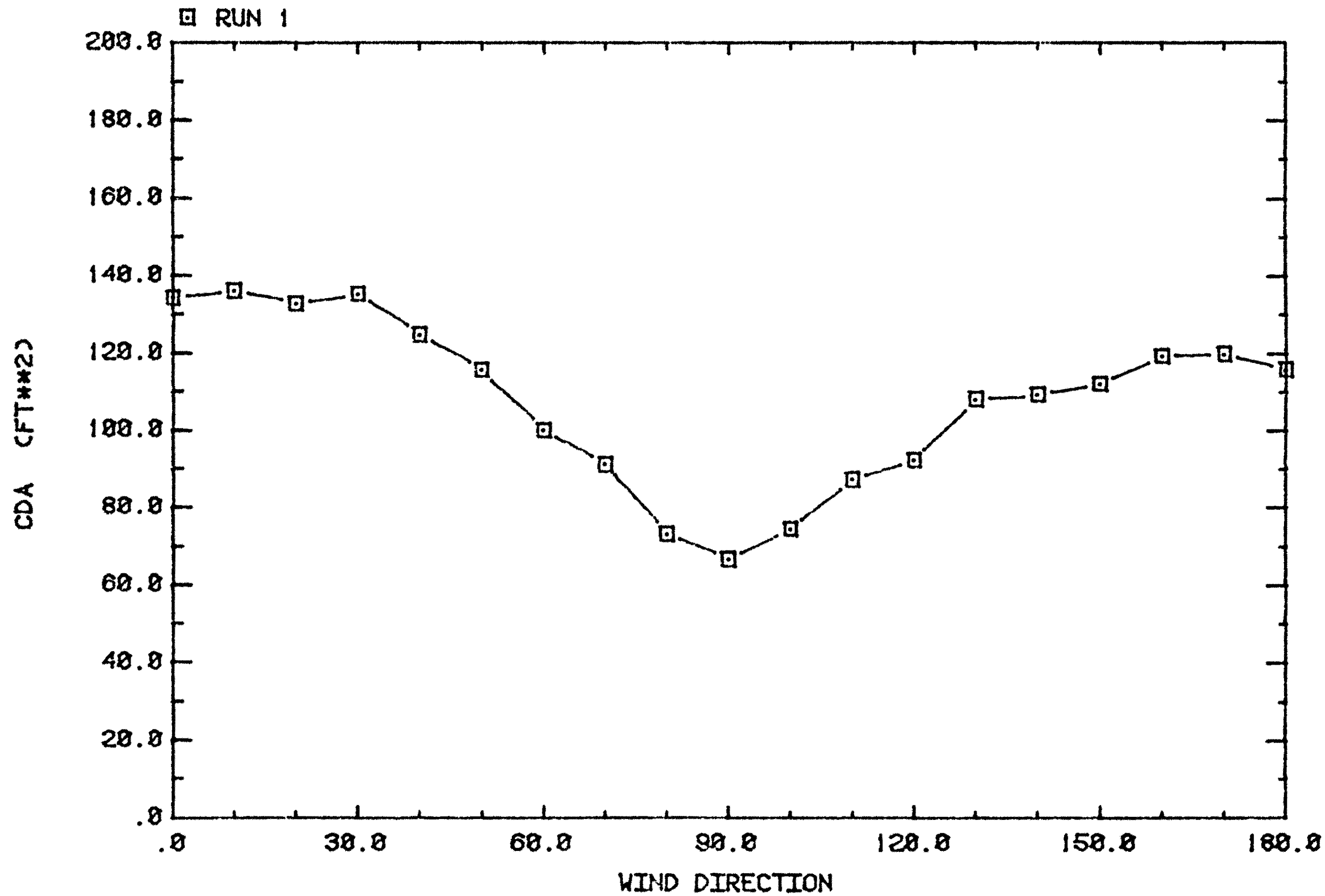

Figure 8. C_DA of Modified Gabrial Antenna--Run 1

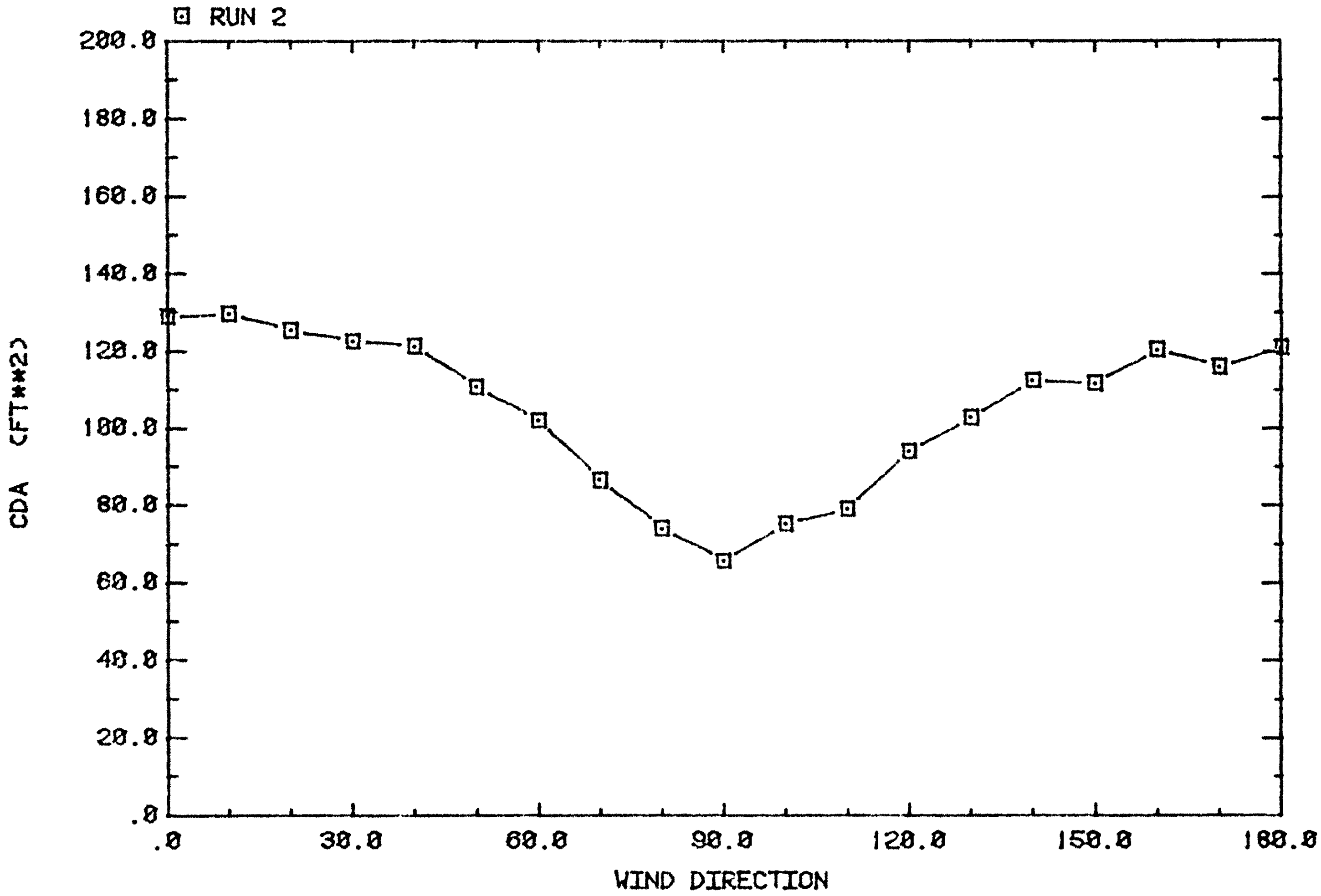

Figure 9. $C_D A$ of Modified Gabrial Antenna--Run 2

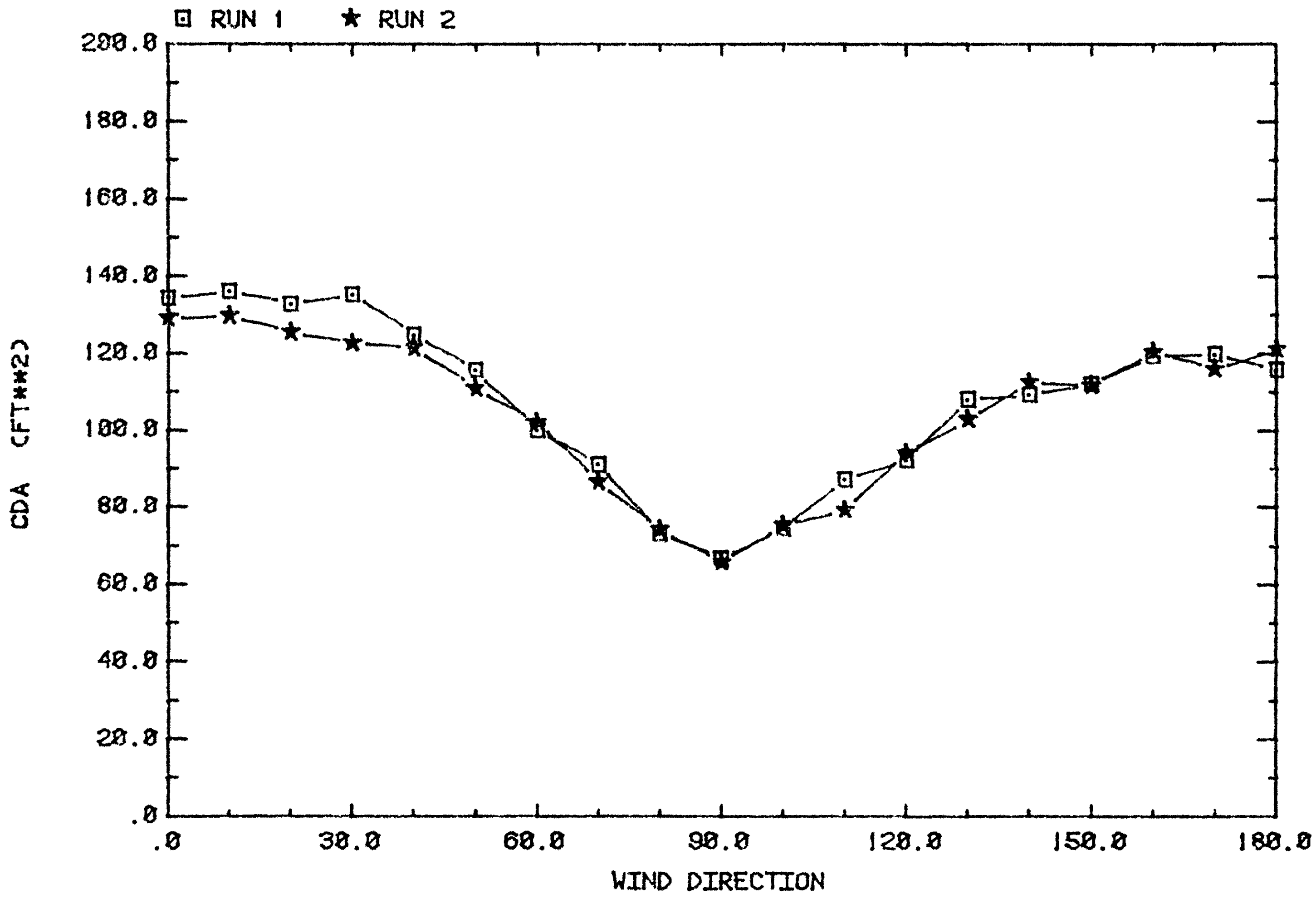

Figure 10. C_DA of Modified Gabrial Antenna--Run 1 and 2

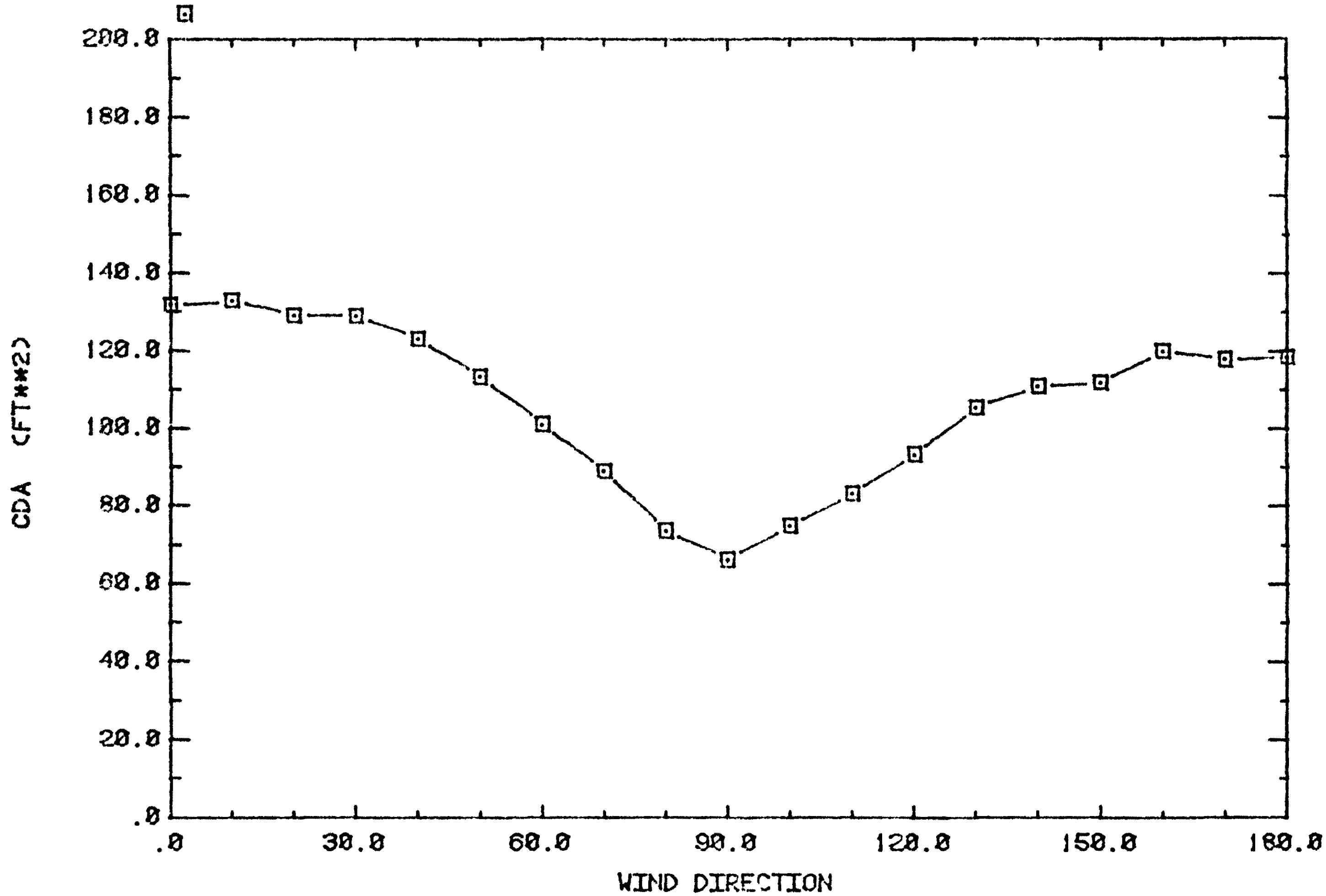

Figure 11. Average C_DA of Modified Gabrial Antenna

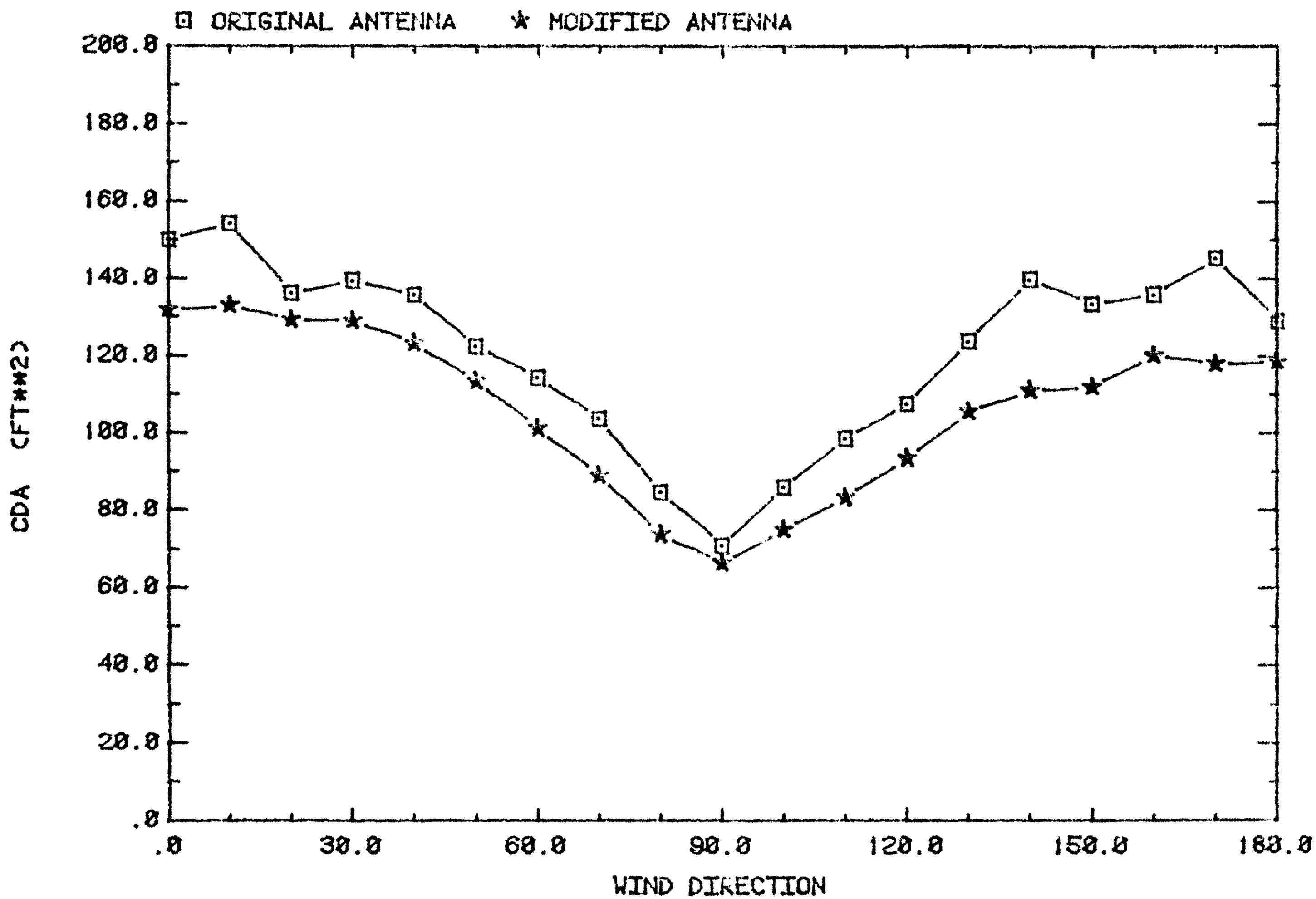

Figure 12. $C_D A$ of Modified and Original Gabrial Antenna

TABLES

Table 1. Drag Force on the Modified Antenna--Run 1

WIND	CD	AREA(SQ.FT)	CDA
0.0	.965	139.4	134.5
10.0	.925	147.3	136.2
20.0	.875	151.8	132.8
30.0	.878	154.1	135.3
40.0	.817	152.8	124.8
50.0	.774	149.4	115.6
60.0	.700	142.8	99.9
70.0	.684	133.3	91.2
80.0	.604	121.2	73.3
90.0	.627	106.5	66.7
100.0	.615	121.2	74.6
110.0	.655	133.3	87.3
120.0	.647	142.8	92.4
130.0	.723	149.4	108.1
140.0	.715	152.8	109.3
150.0	.726	154.1	111.9
160.0	.786	151.8	119.3
170.0	.813	147.3	119.8
180.0	.830	139.4	115.7

Table 2. Drag Force on the Modified Antenna--Run 2

WIND	CD	AREA(SQ.FT)	CDA
0.0	.926	139.4	129.1
10.0	.881	147.3	129.7
20.0	.827	151.8	125.5
30.0	.796	154.1	122.7
40.0	.795	152.8	121.4
50.0	.742	149.4	110.8
60.0	.715	142.8	102.1
70.0	.650	133.3	86.6
80.0	.612	121.2	74.1
90.0	.617	106.5	65.7
100.0	.622	121.2	75.3
110.0	.595	133.3	79.3
120.0	.660	142.8	94.2
130.0	.689	149.4	102.9
140.0	.736	152.8	112.4
150.0	.724	154.1	111.6
160.0	.794	151.8	120.5
170.0	.787	147.3	115.9
180.0	.868	139.4	121.0

Table 3. Drag Force on the Original Antenna

WIND	CD	AREA(SQ.FT)	CDA
0.0	1.076	139.4	150.1
10.0	1.047	147.3	154.2
20.0	.897	151.8	136.1
30.0	.905	154.1	139.4
40.0	.888	152.8	135.7
50.0	.819	149.4	122.3
60.0	.800	142.8	114.2
70.0	.777	133.3	103.6
80.0	.699	121.2	84.7
90.0	.665	106.5	70.8
100.0	.709	121.2	85.9
110.0	.740	133.3	98.6
120.0	.752	142.8	107.4
130.0	.828	149.4	123.7
140.0	.914	152.8	139.7
150.0	.865	154.1	133.3
160.0	.895	151.8	135.8
170.0	.986	147.3	145.3
180.0	.924	139.4	128.9